NAL TR-628T

UDC 662.61

TECHNICAL REPORT OF NATIONAL AEROSPACE LABORATORY

TR-628T

A Numerical Approach to Fuel Droplet Ignition

Takashi NIIOKA, Shinichi ISHIGŪRO, and Takeo SAITOH

September 1980

NATIONAL AEROSPACE LABORATORY

CHŌFU, TOKYO, JAPAN

A Numerical Approach to Fuel Droplet Ignition*

Takashi NIIOKA**, Shinichi ISHIGURO***, and Takeo SAITOH***

ABSTRACT

Ignition time of a fuel droplet suddenly placed in a hot oxidant atmosphere is calculated numerically. Solutions derived from the unsteady equation set, show a characteristic temperature and concentration variation with time, prior to ignition. Ignition time increases as droplet size increases for a droplet initially at room temperature, but not for one of high initial temperature. Although the ignition time of a semi-infinite condensed fuel generally diverges to the infinity in the vicinity of the ignitable limit, the limit of a droplet appears rather suddenly when the ambient temperature drops or droplet diameter decreases. In addition, the effect of a small amount of fuel-vapor fraction in a hot oxidant atmosphere is investigated.

概　　要

単一燃料液滴が高温酸化剤雰囲気に瞬時におかれたときの発火時間が数値的に求められた。従来，準定常解によって議論されてきたが，ここでは非定常方程式を解くことによって，発火前の温度および濃度分布の特徴的な変化をとらえることができた。発火時間は，液滴粒径を大きくすれば増加するが，液滴の初期温度が高くなってくると，この傾向が逆転する。一般に，半無限空間を占める凝縮体の表面での発火時間は，発火限界近くで無限大に発散するけれども，液滴の場合は，雰囲気温度を下げたり粒径を減少させたりするとほとんど突然に限界に達してしまう。この他，高温酸化剤雰囲気内に少量の燃料蒸気が存在するときの発火時間に対する影響についても調べられた。

INTRODUCTION

Although researchers have been grappling with the problem of fuel droplet burning for three decades, important problems remain. In recent years the unsteady effect is often studied, but the fuel droplet ignition process is still unclear even qualitatively. For instance, it is difficult to give a definite answer to the question whether or not larger droplets ignite faster.

The quasi-steady model simplifies the problem of droplet burning and is useful in judging ignition under a given condition. For example, since there is no solution for a diffusion flame stabilized around a droplet of less than a critical diameter, ignition does not occur, and this can be deduced by quasi-steady analysis (e.g., Tarifa et al.[1], Peskin and Wise[2], Jain and Ramani[3], Annamalai and Durbetaki[4], Law[5], and Saitoh[6]). However, in order to calculate ignition time, we must return principally to original unsteady analysis. Bloshenko et al.[7] and Birchley and Riley[8] calculated the unsteady equation set numerically and examined the transient phenomenon of a droplet quickly immersed in a hot oxidant gas. These calculations were made for one case only and various effects on ignition time were not given. Much information can be found in the paper by Faeth and Olson[9], although the chemical reaction in the gas-phase, prior to ignition, is considered to be small perturbations.

It is more difficult to measure ignition time. Although there are some techniques for observing the ignition process (e.g., Nishiwaki[10], El-Wakil and Abdou[11], Faeth and Olson[9], Wood and Rosser[12] and Sangiovanni and Kesten[13], all aspects of ignition time have not been arranged systematically. Each study is limited to a narrow droplet diameter region

* Received August 6, 1980.

** Kakuda Branch

*** Tohoku University

and there are questionable results which differ qualitatively from other data.

Recently Sangiovanni and Kesten[13] and Law[14] solved ignition delay time systematically by coupling quasi-steady solution with an analysis of the droplet-heating process. Because the transient process can not be examined by such treatment, as yet there is no confirmation of the validity of quasi-steadiness in the gas-phase. Since the quasi-steady model tends to yield ignition position at a longer distance from the droplet surface, a great effect on ignition time may occur. In Law's analysis, however, ignition times can be obtained with only elementary functions and his results are convenient in directly inferring effects on ignition time. The dependence on droplet size was first computed parametrically and then definitely explained.

In this paper the unsteady equation set for a fuel droplet suddenly placed in a hot oxidant atmosphere is solved numerically. Although the basic formulation follows Bloshenko et al.[7], ours is the first presentation giving the general tendency of ignition time computed from a full set of equations. A transformation useful for solving the moving boundary problem is adopted and various dependences upon ignition are systematically calculated by the finite-difference method. Computation is performed for n-heptane droplets in air.

FORMULATION

Consider a fuel droplet quickly placed in a stationary hot gaseous oxidant as shown in Figure 1. The irreversible overall one-step reaction $\nu_O O + \nu_F F \rightarrow \nu_P P$ and the first-order reaction, with respect to fuel and oxidizer concentrations, were assumed. Furthermore, it is assumed that the spherical symmetry holds, pressure is constant in the relevant field and radiation effect is negligible. Making an approximation of constant average molecular weight and its properties and disregarding the Dufour-Soret effect, the set of equations governing the system under consideration is as follows:

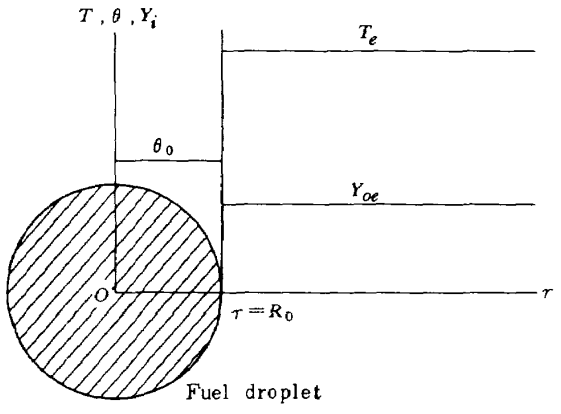

Figure 1 Schematic explanation of the problem.

for liquid-phase $(r < R(t))$

$$\frac{\partial \theta}{\partial t} = a_l \frac{1}{r^2} \frac{\partial}{\partial r}\left(r^2 \frac{\partial \theta}{\partial r}\right), \tag{1}$$

for gas-phase $(r > R(t))$

$$\frac{\partial \rho}{\partial t} + \frac{1}{r^2}\frac{\partial}{\partial r}(r^2 \rho v) = 0, \tag{2}$$

$$\rho c_p \frac{\partial T}{\partial t} + \rho c_p v \frac{\partial T}{\partial r} = \frac{1}{r^2}\frac{\partial}{\partial r}\left(k r^2 \frac{\partial T}{\partial r}\right) + \nu_F M_F Q \dot{w}, \tag{3}$$

$$\rho \frac{\partial Y_i}{\partial t} + \rho v \frac{\partial Y_i}{\partial r} = \frac{1}{r^2}\frac{\partial}{\partial r}\left(\rho D r^2 \frac{\partial Y_i}{\partial r}\right) - \nu_i M_i \dot{w} \quad (i = O \text{ or } F), \tag{4}$$

where the Arrhenius kinetics is written as

$$\dot{w} = \frac{K \rho^2 Y_O Y_F}{M_O M_F} \exp\left(-\frac{E}{\mathcal{R}T}\right). \tag{5}$$

The symbols are defined in the list of nomenclature. The initial and boundary conditions are

$$\theta = \theta_0, \quad \text{at} \quad t = 0, \ r < R(t) \tag{6}$$

$$T = T_e, \ Y_F = 0, \ Y_O = Y_{Oe} \text{ and } v = 0, \quad \text{at} \quad t = 0, \ r > R(t) \quad \text{and} \quad t > 0, \ r \rightarrow \infty \tag{7}$$

$$\frac{\partial \theta}{\partial r} = 0, \quad \text{at} \quad r = 0 \tag{8}$$

$$\left.\begin{aligned} &\theta = T && (9)\\ &\rho_l L \frac{dR}{dt} = k_l \frac{\partial \theta}{\partial r} - k \frac{\partial T}{\partial r}, && (10)\\ &-\rho D \frac{\partial Y_F}{\partial r} = \rho v_w (1 - Y_{Fw}), && (11)\\ &\rho D \frac{\partial Y_O}{\partial r} = \rho v_w Y_{Ow}, && (12)\\ &v_w = \frac{dR}{dt}\left(1 - \frac{\rho_l}{\rho}\right) \quad \text{and} && (13)\\ &Y_{Fw} = \exp\left\{-\frac{M_F L}{\mathcal{R}T_b}\left(\frac{T_b}{T_w} - 1\right)\right\} && (14) \end{aligned}\right\} \text{ at } r = R(t)$$

The last Clausius-Clapeyron's equation is taken to hold good at all times. In nondimensionalizing these equations, the properties are taken to be constant for simplicity. To immobilize the droplet surface and to perform effective computation, the new variables $\xi = r/R\ (t)$ for $r < R\ (t)$ and $\eta = \ln\ (r/R\ (t)) = \ln\xi$ for $r > R\ (t)$ are introduced. The transformation yields[6],

for $\xi < 1\ (r^+ < R^+\ (t^+))$

$$\frac{\partial\theta^+}{\partial t^+} = a^+ \frac{1}{R^{+2}} \frac{\partial^2\theta^+}{\partial\xi^2} + \left(\frac{\xi \dot{R}^{+2}}{R^+} + \frac{a^+}{R^{+2}} \cdot \frac{2}{\xi}\right) \frac{\partial\theta^+}{\partial\xi} \tag{15}$$

for $\eta > 0\ (r^+ > R^+\ (t^+))$

$$\mathscr{L}\{T^+,\ 1,\ -1\} = 0,\ \mathscr{L}\{Y_i,\ L_e,\ 1\} = 0, \tag{16)(17}$$

where operator $\mathscr{L}$ represents

$$\mathscr{L}\{\mathcal{Q},\ m,\ n\} = \frac{\partial\mathcal{Q}}{\partial t^+} - \frac{1}{(R^+ e^\eta)^2} \frac{\partial^2\mathcal{Q}}{\partial\eta^2} - \left(\frac{1}{m(R^+ e^\eta)^2} + \frac{\dot{R}^+}{R^+} - \frac{v^+}{R^+ e^\eta}\right) \frac{\partial\mathcal{Q}}{\partial\eta} + nD_1 Y_o^+ Y_F^+ \exp\left(-\frac{E^+}{T^+}\right) \tag{18}$$

and the dot of $\dot{R}^+$ represents differentiation in respect to t^+. Also, Eq. (2) produces the relation $v^+ = v_w^+ \exp(-2\eta)$. The initial and boundary conditions in nondimensional form are

$$\theta^+ = \theta_0^+, \qquad \text{at} \quad t = 0,\ \xi < 1 \tag{19}$$

$$T^+ = T_e^+,\ Y_F^+ = 0,\ Y_o^+ = Y_{oe}^+ \text{ and } v^+ = 0, \quad \text{at} \quad t = 0,\ \eta > 0 \quad \text{and} \quad t > 0,\ \eta \to \infty \tag{20}$$

$$\frac{\partial\theta^+}{\partial\xi} = 0, \qquad \text{at} \quad \xi = 0 \tag{21}$$

$$\left.\begin{aligned} &\theta_w^+ = T_w^+ && (22)\\ &\frac{dR^+}{dt^+} = \frac{St}{R^+}\left[k^+ \frac{\partial\theta^+}{\partial\xi} - \frac{\partial T^+}{\partial\eta}\right] && (23)\\ &-\frac{\partial Y_F^+}{\partial\eta} = L_e R^+ v_w^+ (\alpha_F - Y_{Fw}^+) && (24)\\ &\frac{\partial Y_o^+}{\partial\eta} = L_e R^+ v_w^+ Y_{ow}^+ && (25) \end{aligned}\right\} \text{at } \xi = 1$$

$$v_w^+ = \frac{dR^+}{dt^+}(1 - \rho^+) \tag{26}$$

and

$$Y_{Fw}^+ = \alpha_F \exp\left\{-L^+\left(\frac{T_b^+}{T_w^+} - 1\right)\right\} \tag{27}$$

The first Damkohler number is defined as

$$D_1 = \frac{K\rho\nu_o\nu_F R_0^2}{a\ (\nu_o M_o + \nu_F M_F)} \tag{28}$$

which is proportional to the square of the initial droplet radius.

CALCULATION PROCEDURE

Numerical calculations were carried out by transforming the above-mentioned equations into implicit finite-difference forms. First the initial and boundary values (θ_0, T_e, Y_{oe} and D_1) were given and the surface temperature (T_w) was assumed. Iteration for integrating the equations was continued until the derived surface temperature was consistent with the assumed value. The mesh sizes of time and space were changed according to ignition time and/or atmospheric temperature to save computing time. Error was kept within the thickness of the resulting curves.

The following data were used for computations of n-heptane; $L_e = 1$, $\alpha_F = 4.51$, $\alpha_O = 1.29$, $E = 20$ Kcal/mole, $L = 75.4$ cal/g, $Q = 10650$ cal/g, $T_b = 98.4°C$, $c_{p\ell} = 0.51$ cal/g°K, $\rho_\ell = 0.68$ g/cm^3 and $k_\ell = 3 \times 10^{-4}$ cal/cmsec°K. The properties in the gas-phase were varied according to the atmospheric temperature. For instance the values for air of $T_e = 600°C$ are $c_p = 0.265$ cal/g°K, $\rho = 4.05 \times 10^{-4}$ g/cm^3 and $k = 1.35 \times 10^{-4}$ cal/cmsec°K.

The history of the maximum temperature (T_m^+) in gas-phase was plotted to determine the moment of ignition and the first inflection point in the $T_m^+ - t^+$ curve was adopted as ignition time. After ignition the envelope diffusion flame develops and combustion proceeds. The behavior of the maximum temperature histories was unstable in this transient region. In certain cases the temperature rose to an impossibly high value, or else the temperature oscillated with time. If we wish to examine the transient region from ignition to combustion in detail, the mesh size must be fine because both temperature and concentration change remarkably near the diffusion flame. The

results up to ignition for this calculation are shown and discussed in the next section.

RESULTS AND DISCUSSION

Figure 2 (a) shows a typical change of temperature profile with time and Figure 2 (b) the corresponding concentration profile. In addition the variation of a few values with time is shown in Figure 3. For some time after being placed in a hot oxidant gas (approximately $0 < t^+ < 10$ in Figure 2), the droplet is heated up while surrounding gas is cooled down. Although a small amount of fuel gas evaporates and diffuses into oxidant gas, an appreciable exothermic reaction does not occur and a temperature larger than the atmospheric temperature (T_e^+) is not found. At $t^+ > 10$ the temperature peak appears at a distance from the surface. As shown in Figure 3, when T_m^+ exceeds T_e^+, surface temperature (T_w^+) and gas-efflux velocity (v_w^+) have an inflection point at $t^+ \approx 10$. After this the maximum temperature position gradually approaches the droplet and T_m^+ increases rapidly prior to ignition. The fuel and oxygen concentration distributions have minimum points near the peak temperature position (η_m). Fuel gas existing in the oxidant side of the minimum point and oxygen gas in the fuel side are consumed promptly and a so-called envelope diffusion flame is established. Therefore the moment of ignition seems to have a premixed-flame aspect. As the activation energy of gas-phase reaction becomes large, the ignition position may move away from the surface and the premixed-flame tendency increases. This is implied by a crack at the ignition of a droplet in hot gas.

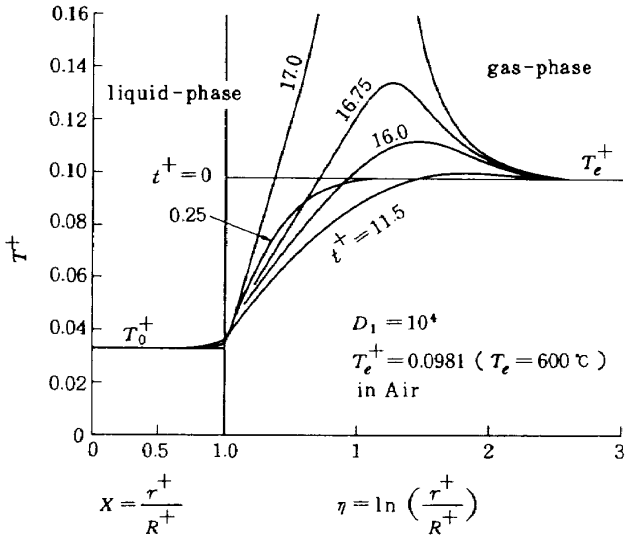

Figure 2 (a) Variation of temperature profile with time.

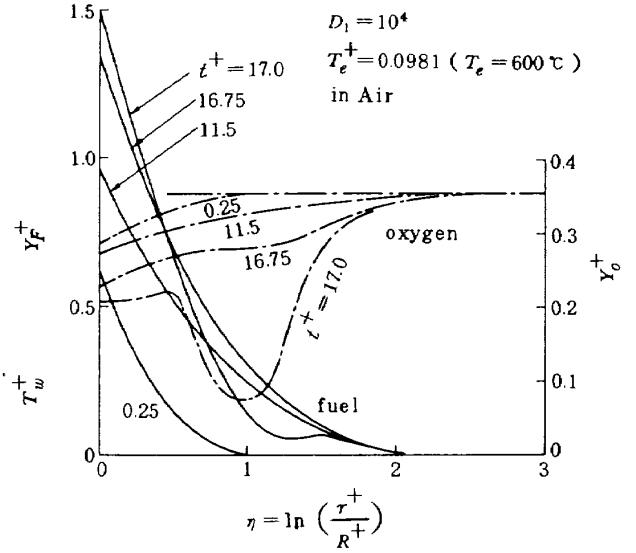

Figure 2 (b) Variation of concentration distribution with time.

Figure 4 illustrates the maximum temperature

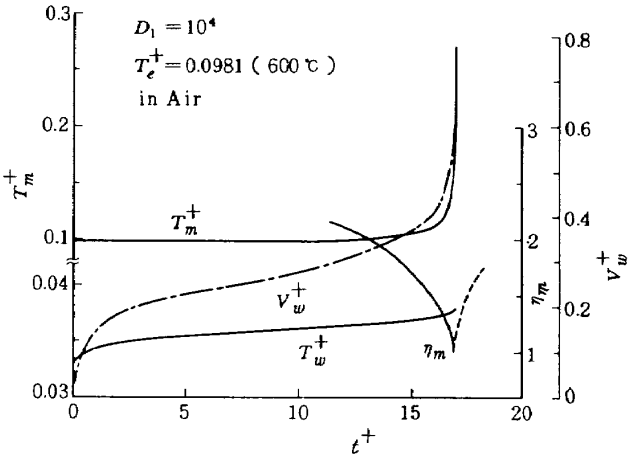

Figure 3 Histories of various values prior to ignition.

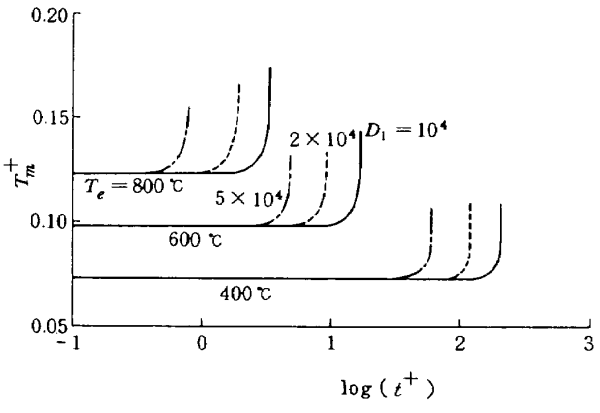

Figure 4 Maximum temperature variation with time.

variation with time for various values of the atmospheric temperature and the Damkohler number. Ignition times are arranged in Figure 5 as a function of the Damkohler number. These figures show that ignition time lengthens when the initial droplet radius (R_0) is large at constant atmospheric temperature. Since the first Damkohler number (D_1) is proportional to R_0^2 and the non-dimensional ignition time (t_{ig}^+) is inversely proportional to R_0^2, the vertical axis of Figure 5 represents non-dimensional ignition time in which the effect of R_0 is eliminated. Although systematic experiments on the effect of droplet size is seldom seen, we can conclude from Figure 5 that Nishiwaki's data[10] and experiments by Faeth and Olson[9] are reasonable and the results by Wood and Rosser[12] are questionable. In their research, Wood and Rosser represent ignition time, based on experimental ignition lag, as a function of external temperature and not of initial diameter.

Past quasi-steady theories have shown that a visible flame can not be observed when the droplet is smaller than a certain critical size. Ignitable limits in Figure 5 indicates this size, i.e. droplets smaller than this limits vaporize completely before ignition. Ignition time is inclined to become slightly longer in the vicinity of the limit.

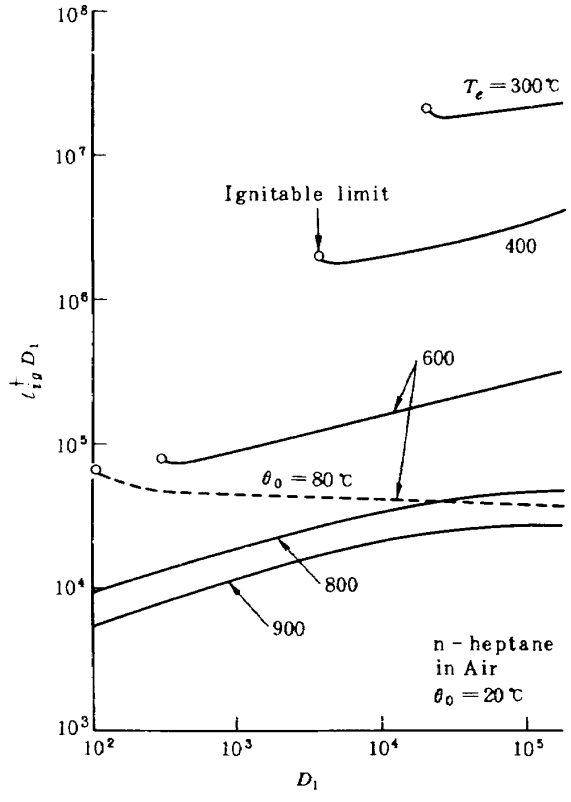

Figure 5 Effect of droplet size on ignition time.

Figure 6 illustrates ignition time as a function of atmospheric temperature. For any droplet size, an ignitable limit exists; ignition can not take place at a temperature lower than this value. Graphical representation of Figures 5 and 6, showing ignition time history up to ignitable limit, is very rare, although critical sizes are usually illustrated as a function of atmospheric temperature. The tendency observed in

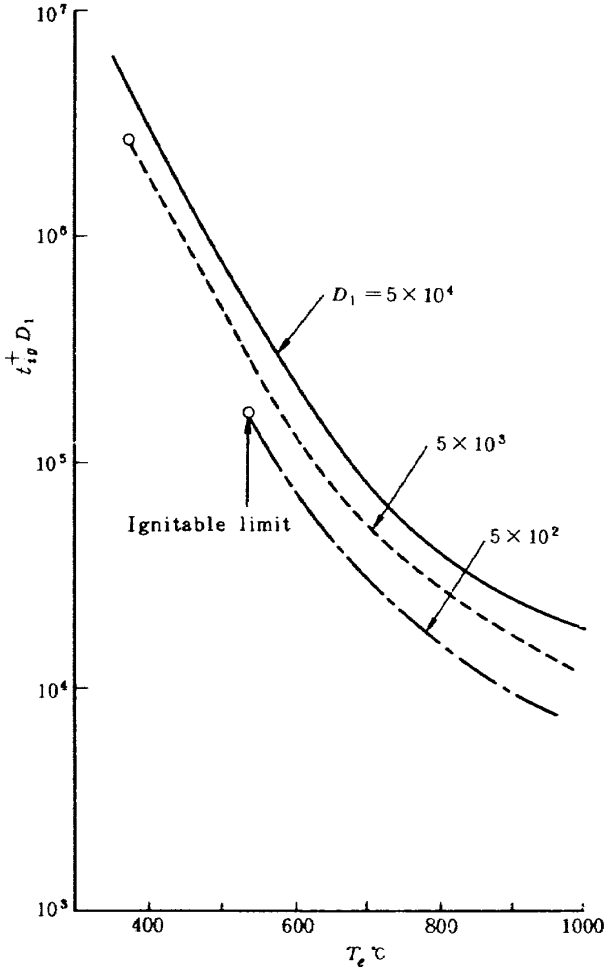

Figure 6 Effect of atmospheric temperature on ignition time.

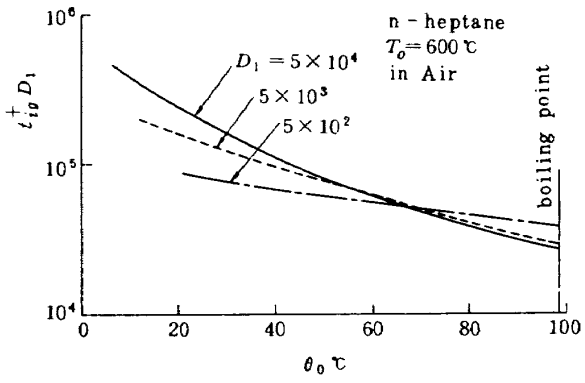

Figure 7 Effect of initial droplet temperature on ignition time.

Figure 5, however, is not always true but depends on the initial temperature of a droplet. This is discussed in Figure 7.

The results in Figures 2 to 6 were obtained for an initial droplet temperature of $\theta_0 = 20°C$. Figure 7 shows the effect of θ_0 for a given droplet size. A smaller droplet ignites faster for $\theta_0 < 60°C$, while a larger droplet ignites faster for $\theta_0 > 70°C$. Therefore it follows that the tendency observed in Figure 5 is not general. When latent heat and the activation energy are not very small, ignition time is divided into two stages, i.e. gasification time and gas-phase reaction time. Droplet-heating time lengthens as the droplet increases in size and therefore fuel-gas evolution time becomes longer. However, if the initial temperature is high, the fuel-gas evolution time approaches zero. Since gas-phase reaction time is short when the Damkohler number is fairly large, ignition time shortens as the droplet increases in size. An example for $\theta_0 = 80°C$ and $T_e = 600°C$ is shown in Figure 5 by the dashed curve. This has not been experimentally observed yet.

The tendency of Figure 8 which represents the effect of oxygen fraction in atmosphere can be easily understood but how is the case of fuel fraction? Figure 9 shows the effect of a small amount of fuel-vapor fraction in a hot oxidant atmosphere. At concentrations less than 0.5%, the ignition process is not very different from a case where no fuel-vapor is present. On the other hand, more than 1% concentration keeps temperature peak from appearing in the relevant transient process and ignition in the external hot mixture takes place faster than droplet ignition. As seen in the figure, a small amount of fuel-vapor reduces the effect of droplet size on ignition time.

The comparison of Law's quasi-steady theory[14] with our calculation was not performed herein, because the evaluation of the gas constant is uncertain in his analysis and therefore the resulting curves are possibly in error. Since ignition time is exponentially affected by the value of the gas constant, the use of undoubtful value causes an unexpected error. Therefore the discussion on the difference between the two will be meaningless.

In the quasi-steady model, the envelope diffusion flame is assumed to exist from the beginning of the analysis. Actually the premixed region builds up at a location much closer the droplet than that of the final diffusion flame and here ignition occurs. The dashed line η_m in Figure 3 implies that the diffusion flame stabilizes at a distance farther from the surface than the location for ignition. A faster reaction rate is needed since flow velocity is larger near the droplet surface. All quantitative differences between the two will arise from the point where ignition occurs. If this is true, it is expected that the quasi-steady model will be successful by correcting only the value of the frequency factor. However, it is suggested contrarily that ignitable limits, near where the interaction between reaction and mass-transfer becomes important over the whole ignition process, differ from each other even qualitatively. Since diffusion flame extinction is discussed in quasi-steady analysis and premixed flame is investigated in the present study,

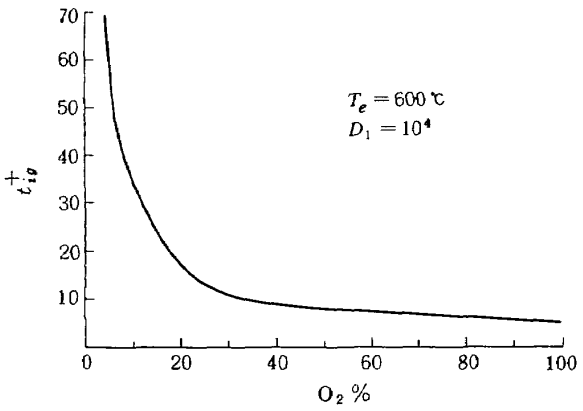

Figure 8 Effect of oxygen fraction in atmosphere on ignition time.

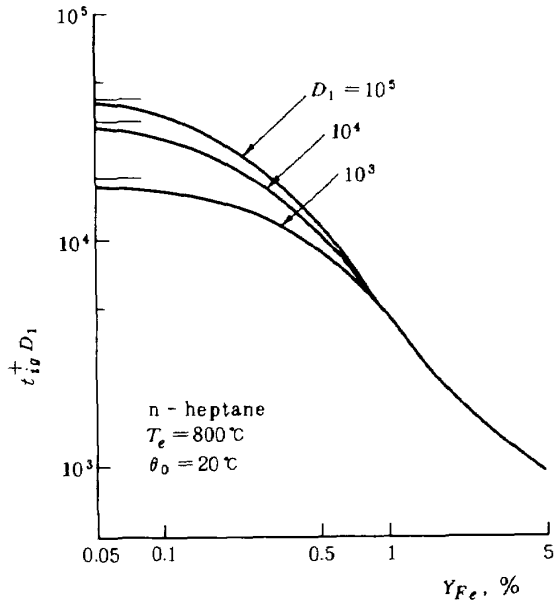

Figure 9 Effect of fuel-vapor fraction in external hot air on ignition time.

large differences of ignitable limits will be produced even if the frequency factor is selected enabling the magnitude of ignition time to fit with the results by Law[14]. The limit derived by quasi-steady analysis would be close to extinction immediately prior to burning out rather than near the ignitable limit.

CONCLUDING REMARKS

A full set of equations for droplet ignition was solved numerically, and the transient behavior of various values and ignition times were obtained, with special attention on droplet size effect. After the external oxygen mixes with evaporating fuel gas, the exothermic reaction of the premixed gas initiates and burns intensely. During this very short transient period minimum points are observed in the oxygen and fuel distributions. The diffusion flame is then established around the minimum points; if the Damkohler number is fairly large, it moves to the location of the stabilized diffusion flame.

It is generally thought that ignition time increases as droplet size becomes large. However, ignition time decreased with droplet size near the ignitable limit. Also, ignition time shortened as the droplet increased in size when the initial temperature of a droplet was higher than 70°C. This is because the gas-phase reaction time becomes short when Damkohler number, proportional to the square of droplet diameter, is large.

Here, results have not been compared with previous experiments for the following reasons: 1), To avoid complexity, our calculation is limited to conduction and convection heat transfer to a droplet, while experimental data are always affected by thermal radiation. The amount of radiation depends on each furnace and therefore estimation is often difficult. 2), Experimental data are limited to a narrow region of droplet size in each experiment. Accordingly, comparison with all aspects shown in Figure 5 is difficult. We must wait for the detailed experimental results to confirm the present calculation. In view of the ready comparison and the parametric discussion, it is of interest to obtain an analytical solution for the unsteady problem as developed by Niioka and Williams[15] for ignition of a condensed material with the surface equilibrium.

NOMENCLATURE

a	thermal diffusivity (cm^2/sec).
a^+	nondimensional thermal diffusivity equal to a_g/a.
c_p	specific heat at constant pressure (cal/g°K).
D	diffusion coefficient (cm^2/sec).
D_1	Damkohler number defined in Eq. (28).
E	activation energy (Kcal/mole).
E^+	nondimensional activation energy equal to $c_p\alpha_f E/\mathcal{R}Q$.
k	thermal conductivity (cal/cm·sec·°K).
k^+	nondimensional thermal conductivity equal to k_g/k.
K	frequency factor (cm^3/mole·sec).
L	latent heat (cal/g).
L^+	nondimensional latent heat equal to $M_F L/\mathcal{R}T_b$.
L_e	Lowis number.
M	molecular weight (g/mole).
Q	heat of reaction (cal/g).
r	radial coordinate (cm).
r^+	nondimensional radial coordinate equal to r/R_0.
R	droplet radius (cm).
R^+	nondimensional droplet radius equal to R/R_0.
$\mathcal{R}$	universal gas constant (cal/mole°K).
S_t	Stefan number equal to $Q_\rho/\alpha_F\rho_g L$.
t	time (sec).
t^+	nondimensional time equal to at/R_0^2.
T	gaseous temperature (°K).
T^+	nondimensional gaseous temperature equal to $c_p\alpha_F T/Q$.
v	radial velocity (cm/sec).
v^+	nondimensional radial velocity equal to $R_0 v/a$.
Y	mass fraction.
Y^+	nondimensional mass fraction equal to $\alpha_i Y_i$.
$\dot{w}$	reaction rate (mole/cm^3sec).
α	nondimensional value equal to $(\nu_O M_O + \nu_F M_F)/\alpha_i M_i$.
η	nondimensional radial coordinate for gas-phase equal to $\ln(r^+/R^+)$.
θ	liquid temperature (°K)
θ^+	nondimensional liquid temperature equal to $c_p\alpha_F\theta/Q$.
ν	number of moles.
ξ	nondimensional radial coordinate for liquid-phase equal to r^+/R^+.
ρ	density (g/cm^3).
ρ^+	nondimensional density equal to ρ_g/ρ.

Subscripts

b boiling point.
e external ($r \to \infty$).
F fuel.
i O or F.
ig ignition.
ℓ liquid (no subscript implies gas-phase).
m value at maximum temperature in gas-phase.
O oxygen.
w surface.
0 initial.

REFERENCES

(1) C. S. Tarifa, P. P. Del Notario and F. G. Moreno; Combustion of Liquid Monopropellants and Bipropellants in Droplets, *Eighth Symposium (International) on Combustion,* William and Wilkins, Baltimore, p. 1035 (1962).

(2) R. L. Peskin and H. Wise; A Theory for Ignition and Deflagration of Fuel Droplet, *AIAA J., 4,* p. 1646 (1966).

(3) V. K. Jain and N. Ramani; Extinction Criterion of a Monopropellant Droplet Burning in an Atmosphere of Inerts, *AIAA J., 7,* p. 567 (1969).

(4) K. Annamalai and P. Durbetaki; Extinction of Spherical Diffusion Flames: Spalding's Approach, *Int. J. Heat Mass Transfer, 17,* p. 1416 (1974).

(5) C. K. Law; Asymptotic Theory for Ignition and Extinction in Droplet Burning, *Comb. Flame, 24,* p. 89 (1975).

(6) T. Saitoh; An Analysis of the Burning of a Single Fuel Droplet via Quasi-Steady Model, *The Technology Reports of the Tohoku University, 43,* p. 47 (1978).

(7) V. N. Bloshenko, A. G. Merzhanov, N. I. Peregudov and B. I. Khaikin; Formation of an Unsteady-State Diffusion Combustion Front with the Ignition of a Droplet of Liquid Fuel, *Fizika Goreniya i Vzryva,* 9, p. 211 (1973).

(8) J. C. Birchley and N. Riley; Transient Evaporation and Combustion of a Composite Water-Oil Droplet, *Comb. Flame, 29,* p. 145 (1977).

(9) G. M. Faeth and D. R. Olson; The Ignition of Hydrocarbon Fuel Droplets in Air, *SAE Transactions, 77,* p. 1793 (1968).

(10) N. Nishiwaki; Kinetics of Liquid Combustion Process: Evaporation and Ignition Lag of Fuel Droplets, *Fifth Symposium (International) on Combustion,* Reinhold, N. Y., p. 148 (1955).

(11) M. M. El-Wakil and M. I. Abdou; The Self-Ignition of Fuel Drops in Heated Air Streams, *Fuel, 45,* p. 177 (1966).

(12) B. J. Wood and W. A. Rosser; An Experimental Study of Fuel Droplet Ignition, *AIAA J., 7,* p. 2288 (1969).

(13) J. J. Sangiovanni and A. S. Kesten; A Theoretical and Experimental Investigation of the Ignition of Fuel Droplets, *Comb. Sci. Tech., 16,* p. 59 (1977).

(14) C. K. Law; Theory of Thermal Ignition in Fuel Droplet Burning, *Comb. Flame, 31,* p. 285 (1978).

(15) T. Niioka and F. A. Williams; Relationship between Theory and Experiment for Radiant Ignition of Solids, *Seventeenth Symposium (International) on Combustion,* The Combustion Institute, Pittsburgh, p. 1163 (1979).

TECHNICAL REPORT OF NATIONAL
AEROSPACE LABORATORY
TR-628T

航空宇宙技術研究所報告628T号（欧文）

昭和55年9月　発行

発行所　航空宇宙技術研究所
東京都調布市深大寺町1880
電話武蔵野三鷹(0422)47-5911(大代表)〒182
印刷所　株式会社　三興印刷
東京都新宿区信濃町12　三河ビル

Published by
NATIONAL AEROSPACE LABORATORY
1,880 Jindaiji, Chōfu, Tokyo
JAPAN